Deleterious Effects of Long-Range Self-Repulsion on the Density Functional Description of O_2 Sticking on Aluminum†

Ester Livshits, Roi Baer,* and Ronnie Kosloff

Institute of Chemistry and the Fritz Haber Center for Molecular Dynamics, the Hebrew University of Jerusalem, Jerusalem 91904 Israel

Received: January 30, 2009; Revised Manuscript Received: April 2, 2009

Density functional theory (DFT) with semilocal functionals such as the local-density and generalized gradients approximations predicts that the dissociative adsorption of oxygen on Al (111) goes through without a barrier in stark contradiction to experimental findings. This problem motivated our study of the reaction of oxygen colliding with a small aluminum cluster Al_5. We found semilocal functionals predict a minute barrier to sticking, associated with smeared long-range charge transfer from the metal to the oxygen. Hybrid B3LYP predicts a larger barrier while the range-separated the Baer−Neuhauser−Livshits (BNL, *Phys. Chem. Chem. Phys.* **2007**, *9*, 2932.) functional finds a more prominent barrier. BNL predicts short-ranged and more abrupt charge transfer from the surface to the oxygen. We conclude that spurious self-repulsion inherent in semilocal functionals causes early electron-transfer, long-range attraction toward the surface and low reaction barriers for these systems. The results indicate that the missing DFT barrier for O_2 sticking on Al (111) may be due to spurious self-repulsion.

I. Introduction

Formation of a metal−oxide layer from an initially clean metal surface and gas phase oxygen molecules is a complex multistep process that differs from metal to metal.[1] Oxidation of metals has been a subject of extensive experimental and theoretical efforts.[2−6] The primary process, common to most metals, is the dissociative adsorption of the oxygen molecule. At a large distance from the surface oxygen is attracted to the metal by weak dispersion forces. For a perfect metal, the attraction is due to of the polarizability of the oxygen molecule. Upon closer approach, a metal electron can attach itself to the approaching oxygen molecule, creating a superoxide, O_2^- adduct. This electron jump causes an increased attraction due to the Coulomb force between the negative charge on the oxygen and its image in the metal. In the gas phase, such an event is known as harpooning.[7] The distance at which harpooning occurs determines the barrier shape and height if any. This distance is affected by the values of the metal work-function and the electron affinity of oxygen. For low work-function metals such as Cs thin films on ruthenium, charge transfer can occur at large distances. For higher work-function metals such as silver and aluminum it is expected to occur later (i,e, at shorter distances). In experiments this is reflected in elevated incident kinetic energy of the oxygen molecule required for sticking.[8]

A considerable amount of information has accumulated on the basis of experimental studies of the oxygen sticking on silver and aluminum surfaces. The importance of charged entities in oxygen sticking (on silver, for example) is seen in spectroscopic studies that have identified molecular ion intermediates in cases where the ionic adducts can be stabilized.[5,9] Gas phase products such as O^- [10] or atomic oxygen[11] have also been identified. Scanning tunneling microscopy (STM) has been employed to identify adsorbed oxygen atoms. In the O_2/Al system the distribution of separation distances between adsorbed oxygen atoms was measured. The surprise is that very large separation distances have been found ranging up to 80 Å.[3,11,12] Additional insight was obtained when the incident energy of the oxygen molecule was varied in a molecular beam experiment. Shorter distances between adatoms were observed for the more energetic oxygen molecules than for the low incident energy oxygen molecules. The low energy oxygen beams showed larger probability for ejection of oxygen atoms into the gas phase.[11,13]

A sound theoretical method is needed for understand and unifying the vast body of experimental observations. If an adiabatic approach is viable here, then density functional theory (DFT) can be employed for obtaining the ground-state potential surface.[6,14] Indeed, the electronic model in DFT is believed to be extremely well-adopted for describing adsorbates on metals.[15] For many oxygen−metal systems there is no activation barrier in accordance with DFT predictions. As pointed out above, experiments indicate that oxygen sticking on aluminum is likely an activated process with a barrier of ∼0.3−0.5 eV.[4] Yet, all extensive high quality DFT calculation for this system[16] fail to identify such an activation barrier.

This sharp discrepancy between DFT predictions and experiment motivated a reassessment of the theory. Behler et al.[17] introduced the concept of local spin-triplet constraint to prevent the electron-transfer process (the latter reduces the spin density on the oxygen molecule). This spin-restricted approach was hailed for its success at treating the O_2 + Al(111) conundrum.[18] However, this method actually raises more questions than it really answers.[19] The concept of local spin restriction has only vague justification in DFT even though it is an effective solution to the problem.

In this paper we demonstrate that the source of error in previous DFT calculations concerning this conundrum is in their use of semilocal functionals, such as the local density and generalized gradients approximation. These functionals suffer from unbalanced treatment of self-repulsion.[20−22] We show that self-repulsion induces a partial transfer of electronic charge from the metal to the oxygen at relatively large distances. The source of self-repulsion is the Hartree energy in the DFT energy that

† Part of the "Robert Benny Gerber Festschrift".

10.1021/jp900892r CCC: $40.75
Published on Web 05/05/2009

is not properly canceled by the local and semilocal exchange−correlation functionals. As we show below, the problem of the barrier for the O_2 + Al system is resolved in a generic way when a functional not suffering from long-range self-repulsion is used. In particular, there is no need for specialized treatments such as local spin restriction.

We demonstrate out case on the O_2 + Al_5 system. Mosch et al.[23] have recently shown that such clusters can be used as reasonable models for the aluminum surface. They also showed that rigorous wave function methods such as CAS-SCF and MRCI predict a barrier for the O_2 + Al_4 system. Carbogno et al.[24] employed these ideas in a dynamical nonadiabatic model. We compare here the PES and character of the charge transfer as predicted by three functionals: the semilocal Perdew−Burke−Ernzerhof (PBE) functional[25] predicts a very small barrier, the hybrid Becke−Lee−Yang−Parr functional (B3LYP),[26] which has a small part of self-repulsion removed, predicts a larger barrier, and the Baer−Neuhauser−Livshits (BNL) range-separated hybrid functional,[22,27,28] which is long-range self-repulsion free,[29,30] predicts an even larger barrier. A brief review of the BNL approach is given in section II. The calculation results are presented in section III and finally, a discussion of these results is presented in the last section.

II. BNL Range Separated Hybrid

For completeness, we describe briefly the BNL functional. In DFT the correlation energy is defined as[31]

$$E_C = T - T_S + U - U_S \tag{2.1}$$

where all quantities are functionals of the ground-state density $n(\mathbf{r})$ in the following way. The density uniquely defines the ground-state wave function ψ of a system of electrons, henceforth called the "interacting system". It also determines unambiguously the ground-state wave function ψ_S of a system of noninteracting fermions having the electron mass, henceforth called the "noninteracting system". In eq 2.1 T is the expectation value of kinetic energy in the interacting system. U is the expectation value of the electron repulsion energy

$$\hat{U} = \frac{1}{2}\sum_{n\neq m} u(\mathbf{r}_n - \mathbf{r}_m) \qquad u(\mathbf{r}) = \frac{1}{r} \tag{2.2}$$

in the interacting system. Finally, T_S and U_S are the expectation values of these operators in the noninteracting system. The correlation energy can also be written as a difference between the expectation values of an interaction. One can write:[22]

$$E_C = \langle\psi|Y_\gamma|\psi\rangle - \langle\psi_S|Y_\gamma|\psi_S\rangle \tag{2.3}$$

where

$$\hat{Y}_\gamma = \frac{1}{2}\sum_{n\neq m} y_\gamma(\mathbf{r}_n - \mathbf{r}_m) \tag{2.4}$$

and $y(\mathbf{r})$ an interaction function, for example:

$$\begin{aligned} y_\gamma(\mathbf{r}) &= \frac{e^{-\gamma r}}{r} \qquad (\text{"Yukawa"}) \\ y_\gamma(\mathbf{r}) &= \frac{\mathrm{erf}[\gamma r]}{r} \qquad (\text{"Erf"}) \end{aligned} \tag{2.5}$$

and other possibilities exist as well.[32] The right-hand side of eq 2.3 is equal to zero when $\gamma \to \infty$ and to $U - U_S$ when $\gamma = 0$. Since $U - U_S \leq E_C \leq 0$,[33] there exists a value of $\gamma > 0$ for which eq 2.3 holds. This value will in general depend on the density; i.e., it is a density functional. The correct selection of the parameter γ is an open issue, and some progress has been made recently.[27,28,34] A practical approach is to select it as a empirical constant.[22,30,35] The correlation energy of eq 2.3 can be written as

$$E_C = [\langle\psi|Y_\gamma|\psi\rangle - E_H^\gamma] - K_X^\gamma \tag{2.6}$$

where

$$\begin{aligned} E_H^\gamma &= \frac{1}{2}\int\int n(\mathbf{r})\, n(\mathbf{r}')\, y_\gamma(\mathbf{r}-\mathbf{r}')\, d^3r\, d^3r' \\ K_X^\gamma &= -\frac{1}{2}\int\int P[n](\mathbf{r},\mathbf{r}')\, y_\gamma(\mathbf{r}-\mathbf{r}')\, d^3r\, d^3r' \end{aligned} \tag{2.7}$$

are the Hartree and exchange energies with respect to the interaction $y_\gamma(\mathbf{r})$ and $P[n](\mathbf{r},\mathbf{r}')$ is the density matrix of noninteracting particles with density $n(\mathbf{r})$. The term in parentheses in eq 2.6 is in not known precisely and is approximated by the BNL correlation functional:[27]

$$[\langle\psi|Y_\gamma|\psi\rangle - E_H^\gamma] \approx E_C^{LYP} + (1-w)\varepsilon_X^\gamma \tag{2.8}$$

with $y_\gamma(\mathbf{r})$ taken as "erf" and ε_X^γ is given elsewhere,[36] and w = 0.1, $\gamma = 0.5a_0^{-1}$ are empirical parameters.[27]

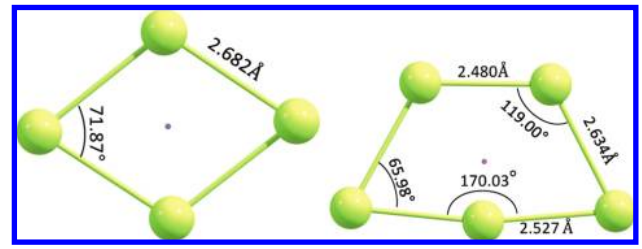

Figure 1. Optimized geometry of the planar Al_4 and Al_5 clusters used in the present study. The dot in the center indicates the Z axis along which the oxygen atom or the perpendicular dioxygen molecule approaches.

TABLE 1: Ionization Energies for the Al Clusters in the Different Functionals (LANL2DZ Basis Set)

		ionization potential (eV)	
cluster	functional	ΔSCF	$-\varepsilon_{HOMO}$
Al_4	PBE	6.6	4.3
	B3LYP	6.6	4.8
	BNL	6.6	6.6
Al_5	PBE	6.7	4.7
	B3LYP	6.7	5.1
	BNL	6.4	6.7

III. Results

In this section we study the interaction of oxygen (atom/diatom) with a Al clusters. We focus on the cluster to oxygen electron transfer and on the potential barrier for the reaction, determining their sensitivity to the level of long-range self-repulsion correction in the functional. We present results using the functionals PBE, suffering from self-repulsion, B3LYP which incorporates partial self-repulsion correction and BNL which has a full long-range correction. The calculations were performed using a modified version of the Q-CHEM software.[37] The geometry of the clusters (which is kept fixed on during oxygen approach) is obtained by optimization at the B3LYP/6-311G(2d) level. In the calculation of the cluster-oxygen system the LANL2DZ basis set was used. Our results show that Al_4 and Al_5 clusters prefer a planar structure, as shown in Figure 1, with Al_4 forming a rhombus while Al_5 a distorted trapezoid. These results are in accord with previous works done for the Al_n clusters.[38] The ground electronic state of Al_4 a spin-triplet,

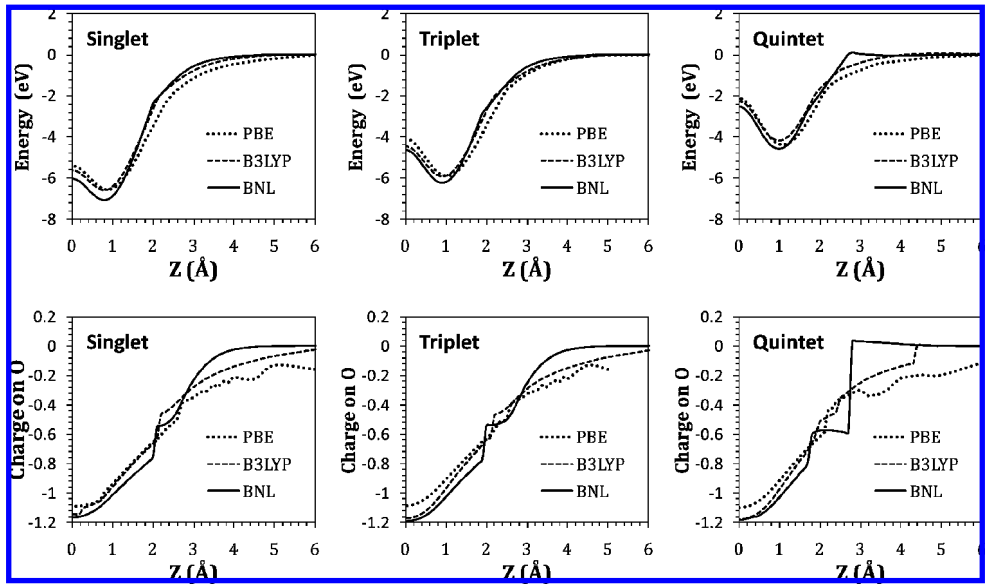

Figure 2. Potential curves (upper panel) and oxygen Mulliken-charge (lower panel) for different spin states of the Al_4 + O system as a function of the coordinate Z using the PBE, B3LYP, and BNL functionals.

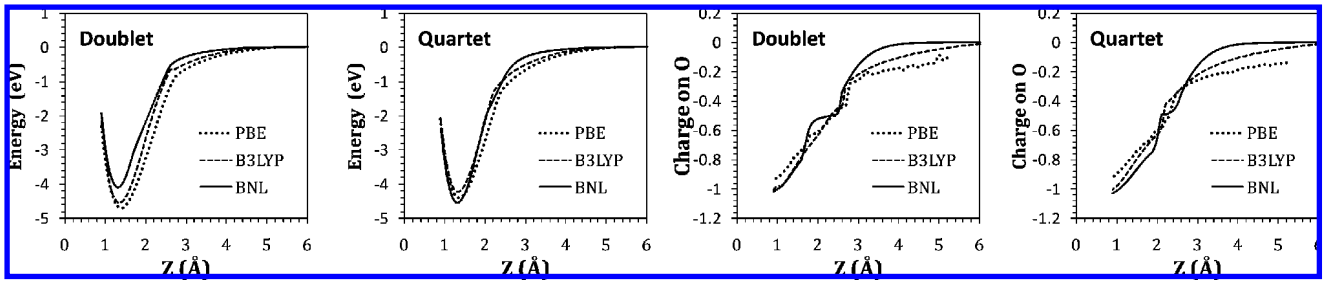

Figure 3. Potential curves (upper panel) and oxygen Mulliken-charge (lower panel) for different spin states of the Al_5 + O system as a function of the coordinate Z using the PBE, B3LYP, and BNL functionals.

which is almost degenerate with the spin singlet, while that of Al_5 is a spin-doublet.

The significant difference between the functionals, dominating the chemistry of the reaction is the metallic "Fermi level". In a metal surface the work function should equal to $-\varepsilon_{Fermi}$ where ε_{Fermi} is the Fermi level (relative to the vacuum).[20] In a cluster the cost of pulling out an electron from the metal is the ionization energy (IP) which should equal $-\varepsilon_{HOMO}$ where ε_{HOMO} is the energy of the highest occupied DFT molecular orbital (HOMO).[39] When approximate functionals are used, this rule is not observed, as seen in Table 1. Indeed, the semilocal PBE functional predicts a ΔSCF IP of 6.6−6.7 eV as the other functionals do while its $-\varepsilon_{HOMO}$ is lower by about 2 eV. B3LYP exhibits a similar problem but to a smaller extent; the difference is ∼1.6 eV. In BNL, where long-range self-repulsion is removed the two quantities are very similar: less than 0.3 eV. The fact that the location of the Fermi level in PBE is 2 eV too high is consequential for the reaction barrier as will be explained in the discussion section below.

A. The O + Al_n system. Both atomic as well as molecular oxygen are electronegative and are thus exposed to electron transfer as they approach the cluster. Since atomic O + Al_n is simpler we start with it. We consider an oxygen atom approaching perpendicular to the plane of the cluster along the Z axis (this axis passes through the dark point at the hollow site in the plane of the cluster shown in Figure 1). Consider first the Al_4 cluster. In the asymptotic channel ($Z \rightarrow \infty$) the Al_4 + O reaction has four possible spin configurations. An O(↑↑) + Al_4(↑↑) quintet, O(↑↑) + Al_4(↑↓) triplet and two singlets: O(↑↑) + Al_4(↓↓) and O(↑↓) + Al_4(↑↓). Assuming the approaching atom is in its ground state (triplet) only the first three of these spin configurations are of interest. In Figure 2 we show the potential curves for the approaching oxygen calculated using the PBE, B3LYP and BNL functionals in the singlet, triplet and quintet states.

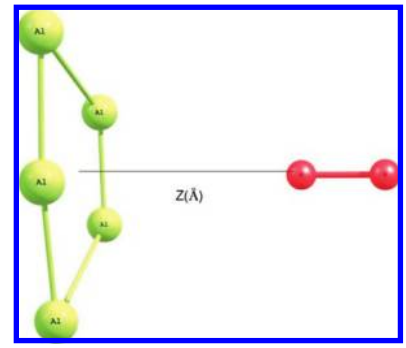

Figure 4. Configuration of an oxygen molecule (red) approaching the planar Al_5 cluster, in perpendicular orientation along the z direction toward the hollow site.

Let us first discuss the singlet potential curve. We find that the BNL curve is sturdier and the attraction of O to the surface starts much later (when the oxygen atom is closer to the surface) than for B3LYP and even more so for PBE. This behavior is related to the way the electron is transferred to the oxygen atom as it approaches the surface, shown in the lower panel of Figure 2. According to PBE the oxygen atom gets noticeable charge at large distances (beyond 6 Å).[40] According to BNL the electron-transfer process starts only when oxygen is considerably

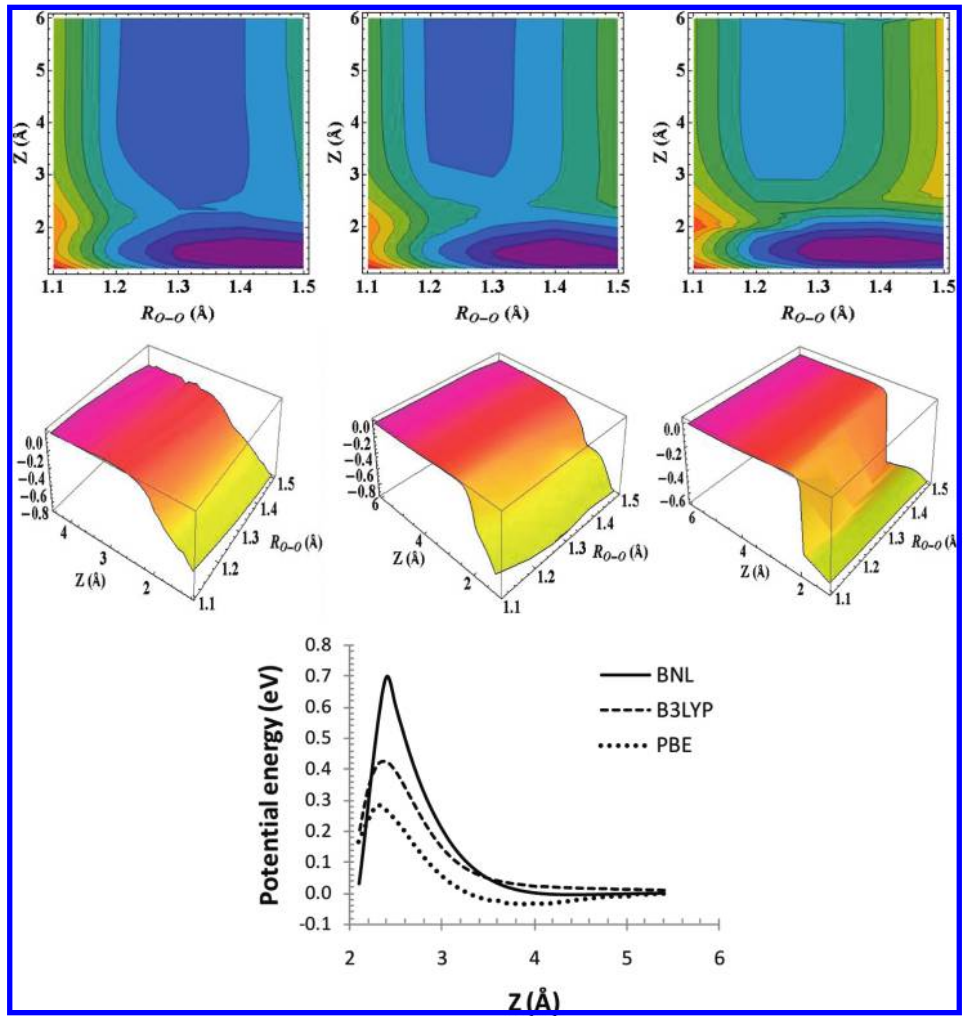

Figure 5. Top panels: isopotential contours (energy difference between contour lines is 0.35 eV) for the for $O_2 + Al_5$ reaction at the quartet state. Middle panels: charge on the oxygen molecule as a function of O−O distance *R* and O-cluster distance *Z*. The functionals used for the calculation are (left to right): PBE, B3LYP, and BNL. Bottom panel: cut through the potential surface at $R = 1.2$Å.

closer, at $Z = 4$ Å. B3LYP is in between: the transfer is still long-range but less so than PBE. The smearing of the electron-transfer process by PBE is typical of functionals that have self-repulsion.[41] Since charged particles are attracted to metals from a distance (due to polarization of the metal surface) the potential curve according to PBE shows attraction already at 6 Å. Accordingly, the BNL curve shows attraction only at 4 Å.

In the triplet state the situation is similar but charge transfers less readily in the PBE calculation. In the quintet state the BNL functional shows a large sharp jump in the charge of oxygen occurring at 2.8 Å. This late electron transfer causes the BNL potential to exhibit a barrier. Such a barrier rises because in the quintet state the high energy electrons in the metal are both "up" spin states just like the two "up"-spin p electrons in the oxygen. Thus the Pauli principle prevents the transfer from the metallic HOMO and the affinity level of the oxygen must further decrease (O must come closer to the metal) so as to allow the transfer from the HOMO−1 metallic level.

A complementary picture is obtained by looking at the amount of charge transferred to the oxygen as a function of *Z* also shown in Figure 2. In both the singlet and triplet states the charge transfer to oxygen grows gradually as it approaches the surface. At a distance of 1.8−2 Å, where a covalent bond is formed, a sharp increase in the transferred charge is seen. Comparing the charge transfer between the three functionals, we see differences in the asymptotic behavior. Seems like the PBE ground state is already partially charged, although severe SCF convergence problems give an erratic curve at large distances. The B3LYP curve seems better; it starts from zero charge transfer at long distances (SCF also converges reliably for B3LYP than for PBE). According to BNL, charge transfer starts at 4 Å. The long-range smearing of charge, even if on a small scale, shows that PBE results are objectionable. This observed behavior is actually typical of self-repulsion: charge is much "too mobile" in DFT calculations suffering from self-repulsion.[20] Finally, let us consider the charge transfer in the quintet state. Here we observe a huge jump at a sharp point in the BNL functional that is not seen in B3LYP and PBE. This jump is indicative of a diabatic crossing between ionic and covalent diabatic curves, as indeed seen in the upper panel.

In Figure 3, we present the potentials and charge-transfer profiles of the $O + Al_5$ system. Here there are two spin states corresponding to triplet oxygen: the doublet $O(\uparrow\uparrow) + Al_5(\downarrow)$ and the quartet $O(\uparrow\uparrow) + Al_5(\uparrow)$. This system is more involved because the differences between the functionals is not only quantitative but also qualitative. The first issue is the relative energetics of the spin states. At the asymptote the spin-doublet and quartet are degenerate. However, at the bonding well minimum they differ. PBE and B3LYP predict that the energies of the two spin states are very similar, with the doublet being slightly lower, by about 0.3 eV. BNL on the other hand they predict that the quartet state is lower in energy, by 0.5 eV. The different spin

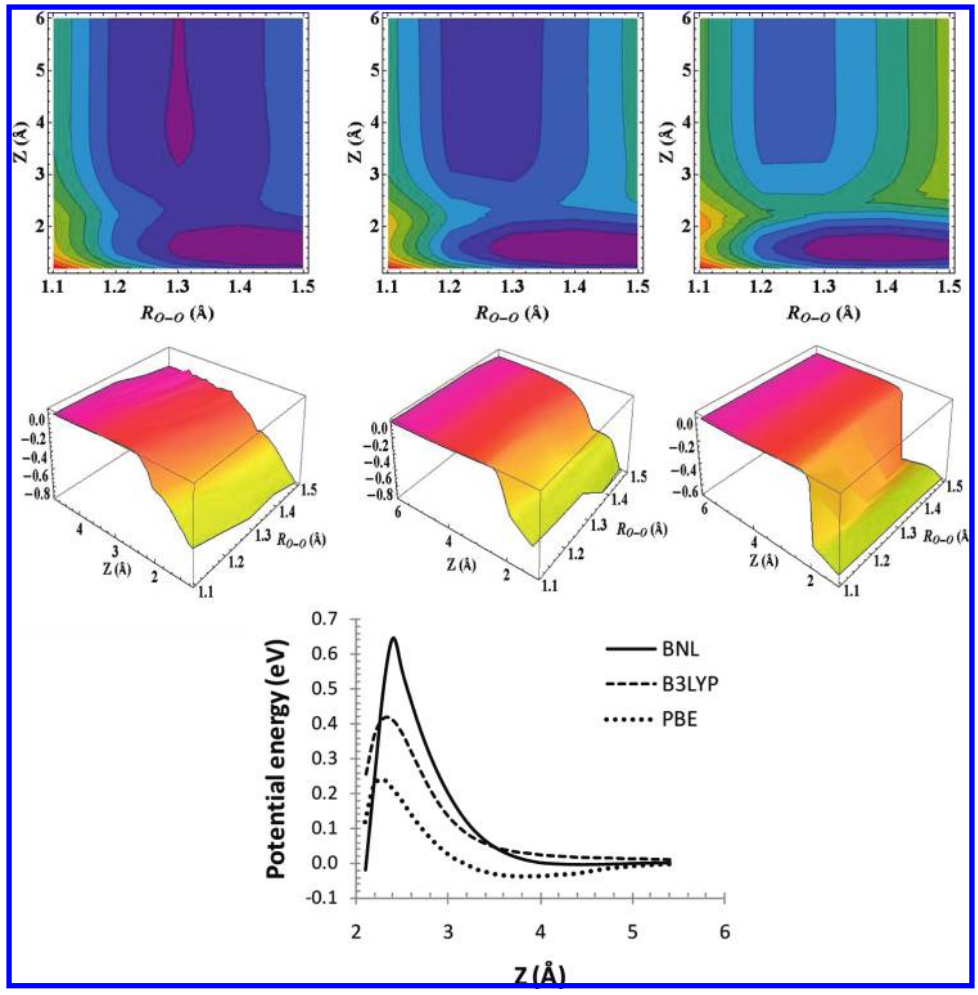

Figure 6. Top panels: isopotential contours (energy difference between contour lines is 0.35 eV) for the for $O_2 + Al_5$ reaction at the quartet state. Middle panels: charge on the oxygen molecule as a function of O−O distance *R* and O-cluster distance *Z*. The functionals used for the calculation are (left to right): PBE, B3LYP, and BNL. Bottom panel: cut through the potential surface at $R = 1.2$Å.

states notwithstanding, the bonding energies for all three functionals are similar: 4.7 eV. This is much smaller than the previous result for Al_4, probably a result of the choice of axis of approach, which is a symmetry axis but most likely is not optimal with respect to Al−O bond formation. In general, the same qualitative features for the mechanism of reaction as observed for the $O + Al_4$ are seen here as well. Here too, charge is transferred much too early in PBE than in B3LYP. In B3LYP charge transfer is smeared and starts beyond 6 Å. On the other hand, in BNL the transfer starts when O is closer, at 3.5 Å.

B. $O_2 + Al_5$ System. We now turn to investigate the molecular oxygen interaction with the Al_5 cluster. Figure 4 shows the perpendicular O_2 molecule as it approaches the central hollow site of the frozen planar Al cluster. *R* is the distance between the two oxygen nuclei and *Z* is the distance of the closest oxygen atom to the cluster plane. The PBE, B3LYP, and BNL calculations were performed for 5 values of *R* and 49 values of *Z*. We considered the spin doublet correlated with $O_2(\uparrow\uparrow) + Al_5(\downarrow)$ and the quartet correlated with $O_2(\uparrow\uparrow) + Al_5(\uparrow)$. All three functionals predict that at the bonding well the doublet state is lower in energy than the quartet state near bonding (the two are degenerate when the $Z \rightarrow \infty$).

Let us first discuss the quartet state (Figure 5). BNL exhibits a potential well at $(Z, R) = \sim(1.5, 1.4)$ Å. This well is lower by 1 eV from the bottom of the broad entrance valley, from which it is separated by a barrier. The saddle point at the barrier is situated at $(Z, R) = \sim(2.2,1.3)$ Å and is 0.5 eV above the incoming potential valley minimum. The low energy release (1 eV) in this reaction is due perpendicular position approach constraint; only one O−Al bond is formed. PBE and B3LYP methods display similar trends, with PBE predicting a somewhat longer O−O bond length while the molecule is bonded to the surface. PBE and B3LYP predict a smaller barrier of 0.2 eV.

The electron-transfer profile is shown in the middle panel of Figure 5 determining the energetics of the reaction. According to PBE a partial transfer occurs early (as far as $Z \approx 4.5$ Å), evidenced in a long-range attraction of O_2 toward the surface (Figure 5 low panel). In BNL the charge transfer is delayed to smaller *Z* and occurs abruptly at $Z = 2.2$ Å. We find the top of the barrier located almost exactly at the charge-transfer point. In B3LYP and BNL there is no evidence for the long-range attraction.

We now discuss the results for the doublet state, which are qualitatively similar to those of the quartet, as shown in Figure 6. The differences are in lower barriers (by about 0.1 eV).

To ensure convergence with respect to basis set, especially since anions are sensitive to this issue, we have repeated some of the calculations using a aug-cc-pVTZ basis set on the oxygen atoms that includes diffuse wave functions. We found that BNL results presented here are essentially unchanged; i.e., the barrier position and height is very close to those presented here.

IV. Summary and Discussion

We have studied the adiabatic potential curves and surfaces (PES) for the $O + Al_n$ ($n = 4, 5$) and $O_2 + Al_5$ reactions using three density functional approaches. The details of the electron-transfer process showed that in both systems the semilocal functionals tend to smear the process of charge transfer over relatively large distances while BNL localizes it. In $O + Al_n$ (Figure 2 and Figure 3) this effect is seen as well but to a lesser extent. The PES derived from the semilocal functional, PBE, showed a small reaction barrier for the $O_2 + Al_5$ reaction while the hybrid functional B3LYP exhibited a larger barrier and the barrier was predicted to be more significant still by the range-separated hybrid BNL.

In Table 1 we showed that the three different functionals predict very different Fermi levels (HOMO energies). This is in spite of the fact that they all give almost the same ionization potential as calculated by the ΔSCF method. The discrepancy between Fermi level and IP is due to the lack of derivative discontinuity,[20] which is associated with self-repulsion.[42] The fact that in PBE and B3LYP the Fermi level is too high by 1.6−2 eV is the main reason for their tendency to predict that charge transfer starts at relatively large distances. The self-repulsion in semilocal functionals is also the cause for the smearing of the electron-transfer process over a large distance interval. One may argue that self-repulsion can work both ways and destabilize the anion as well. This is true but the affinity level of O_2 is only ∼0.4 eV below the vacuum[43] and thus there is not much to be gained by the self-repulsion on O_2. For the $O + Al_n$ reaction, however, the situation is different. The affinity level of O is ∼1.5 eV below the vacuum,[44] and thus there is an effective partial cancelation of self-repulsion errors. This most likely explains the fact that the potential surfaces predicted by the three functionals for the $O + Al_n$ reaction are similar.

DFT has become the primary method for calculating adiabatic potential energy surfaces for molecule−surface encounters. As a consequence, DFT is also defining the qualitative language for describing surface−molecule encounters. It is crucial that DFT be applied with functionals that can treat electron transfer quantitatively, since this is an essential ingredient in any molecule−metal surface interaction. While self-repulsion was identified as the principal cause for the deleterious description of the electron-transfer process by semilocal functionals, it is not self-evident that any method that corrects for self-interaction is automatically applicable. It was recently shown that methods like the Perdew−Zunger self-interaction-correction[45] do not in fact give satisfactory potential surfaces when more than 1 or 2 electrons are present. A typical example given was the Ne_2^+ system where an extra electron (or hole) is shared by distant many-electron systems.[46] The BNL functional does not suffer from this many electron self-interaction problem if the range parameter γ is tuned correctly as recently demonstrated.[28] Despite the success of BNL for molecules and small clusters, its adequacy for bulk metal surfaces is not established especially in view of the presence of long-range exchange. It is therefore a matter for future research, and new ideas, see for example ref 47, to determine how to remove self-interaction in bulk metal surfaces.

The oxygen−aluminum system was chosen here because it has become a challenge to semilocal DFT theory: the prediction of a barrierless reaction was confronted with an apparent significant activation barrier in experiment. We showed that spurious self-repulsion causes small barriers and smearing of electron transfer in semilocal DFT description of these processes on clusters. The functional we used for removing self-repulsion was BNL and it predicted higher barriers and abrupt electron transfer. Since BNL was never tested for bulk metal surfaces it is not possible to make definite predictions for these systems. It is likely, however, that our findings concerning the deleterious effect of self-repulsion on the metal-molecule electron-transfer process hold for bulk surfaces.

Acknowledgment. We gratefully thank the Israel Science Foundation for supporting this research.

References and Notes

(1) (a) Somorjai, G. A. *Introduction to surface chemistry and catalysis*; Wiley: New York, 1994; p xxiv, 667 p; (b) Noguera, C., *Physics and chemistry at oxide surfaces.*, Digitally printed 1st pbk. ed.; Cambridge University Press: Cambridge, New York, 2005; p xv, 223 p.

(2) (a) Greber, T. *Surf. Sci. Rep.* **1997**, *28*, 3–64. (b) Vattuone, L.; Boragno, C.; Pupo, M.; Restelli, P.; Rocca, M.; Valbusa, U. *Phys. Rev. Lett.* **1994**, *72*, 510–513. (c) Reijnen, P. H. F.; Raukema, A.; Vanslooten, U.; Kleyn, A. W. *J. Chem. Phys.* **1991**, *94*, 2368–2369. (d) Spruit, M. E. M.; Kleyn, A. W. *Chem. Phys. Lett.* **1989**, *159*, 342–348. (e) Kasemo, B.; Tornqvist, E.; Norskov, J. K.; Lundqvist, B. I. *Surf. Sci.* **1979**, *89*, 554–565. (f) Kasemo, B. *Phys. Rev. Lett.* **1974**, *32*, 1114–1117. (g) Hellberg, L.; Stromquist, J.; Kasemo, B.; Lundqvist, B. I. *Phys. Rev. Lett.* **1995**, *74*, 4742–4745. (h) Okada, M.; Moritani, K.; Yoshigoe, A.; Teraoka, Y.; Nakanishi, H.; Dino, W. A.; Kasai, H.; Kasai, T. *Chem. Phys.* **2004**, *301*, 315–320. (i) Katz, G.; Zeiri, Y.; Kosloff, R. *Isr. J. Chem.* **2005**, *45*, 27–36. (j) Katz, G.; Kosloff, R.; Zeiri, Y. *J. Chem. Phys.* **2004**, *120*, 3931–3948. (k) Citri, O.; Baer, R.; Kosloff, R. *Surf. Sci.* **1996**, *351*, 24–42. (l) Darling, G. R.; Holloway, S. *Rep. Prog. Phys.* **1995**, *58*, 1595–1672. (m) Gross, A.; Scheffler, M. *Phys. Rev. B* **1998**, *57*, 2493–2506.

(3) Brune, H.; Wintterlin, J.; Behm, R. J.; Ertl, G. *Phys. Rev. Lett.* **1992**, *68*, 624–626.

(4) Osterlund, L.; Zoric, I.; Kasemo, B. *Phys. Rev. B* **1997**, *55*, 15452–15455.

(5) Besenbacher, F.; Norskov, J. K. *Prog. Surf. Sci.* **1993**, *44*, 5–66.

(6) Norskov, J. K.; Scheffler, M.; Toulhoat, H. *MRS Bull.* **2006**, *31*, 669–674.

(7) (a) Polanyi, M.; Ogg, R. A. J. *Trans. Faraday Soc.* **1935**, *31*, 604. (b) Evans, M. G.; Polanyi, M. *Trans. Faraday Soc.* **1938**, *34*, 11.

(8) Kleyn, H. In *Electronic and atomic collisions: proceedings of the 10th International Conference on the Physics of Electronic and Atomic Collisions, Paris, 21−27 July, 1977: invited papers and progress reports*; Watel, G., Ed.; North-Holland Pub. Co.: Amsterdam, New York, 1978; p 451.

(9) (a) Campbell, C. T. *Surf. Sci.* **1986**, *173*, L641–L646. (b) Upton, T. H.; Stevens, P.; Madix, R. J. *J. Chem. Phys.* **1988**, *88*, 3988–3995. (c) Kamath, P. V.; Prabhakaran, K.; Rao, C. N. R. *J. Chem. Soc., Chem. Commun.* **1987**, 715–715. (d) Schmeisser, D.; Demuth, J. E.; Avouris, P. *Chem. Phys. Lett.* **1982**, *87*, 324–326. (e) Bange, K.; Madey, T. E.; Sass, J. K. *Chem. Phys. Lett.* **1985**, *113*, 56–62. (f) Dean, M.; Mckee, A.; Bowker, M. *Surf. Sci.* **1989**, *211*, 1061–1067. (g) Bukhtiyarov, V. I.; Boronin, A. I.; Savchenko, V. I. *Surf. Sci.* **1990**, *232*, L205–L209. (h) Vattuone, L.; Rocca, M.; Valbusa, U. *Surf. Sci.* **1994**, *314*, L904–L908. (i) Gustafsson, K.; Andersson, S. *J. Chem. Phys.* **2004**, *120*, 7750–7754.

(10) Grobecker, R.; Shi, H.; Bludau, H.; Hertel, T.; Greber, T.; Bottcher, A.; Jacobi, K.; Ertl, G. *Phys. Rev. Lett.* **1994**, *72*, 578–581.

(11) (a) Komrowski, A. J.; Sexton, J. Z.; Kummel, A. C.; Binetti, M.; Weisse, O.; Hasselbrink, E. *Phys. Rev. Lett.* **2001**, *8724*, 246103. (b) Binetti, M.; Weisse, O.; Hasselbrink, E.; Komrowski, A. J.; Kummel, A. C. *Faraday Discuss.* **2000**, 313–320.

(12) Brune, H.; Wintterlin, J.; Trost, J.; Ertl, G.; Wiechers, J.; Behm, R. J. *J. Chem. Phys.* **1993**, *99*, 2128–2148.

(13) Binetti, M.; Weisse, O.; Hasselbrink, E.; Katz, G.; Kosloff, R.; Zeiri, Y. *Chem. Phys. Lett.* **2003**, *373*, 366–371.

(14) (a) Bocan, G. A.; Muino, R. D.; Alducin, M.; Busnengo, H. F.; Salin, A. *J. Chem. Phys.* **2008**, *128*, -. (b) Alducin, M.; Busnengo, H. F.; Muino, R. D. *J. Chem. Phys.* **2008**, *129.* (c) Trail, J. R.; Bird, D. M.; Persson, M.; Holloway, S. *J. Chem. Phys.* **2003**, *119*, 4539–4549. (d) Sein, L. T.; Jansen, S. A. *J. Catal.* **2000**, *196*, 207–211. (e) Nakajima, T.; Yamashita, K. *Bull. Chem. Soc. Jpn.* **2001**, *74*, 2279–2283.

(15) Stampfl, C.; Scheffler, M. *Surf. Sci.* **1999**, *433*, 119–126.

(16) (a) Yourdshahyan, Y.; Razaznejad, B.; Lundqvist, B. I. *Sol. Stat. Comm.* **2001**, *117*, 531–535. (b) Lundqvist, B. I.; et al. *Surf. Sci.* **2001**, *493*, 253–270. (c) Kiejna, A.; Lundqvist, B. I. *Phys. Rev. B* **2001**, *6308*, 5405. (d) Hult, E.; Hyldgaard, P.; Rossmeisl, J.; Lundqvist, B. I. *Phys. Rev. B* **2001**, *64*, 195414. (e) Sasaki, T.; Ohno, T. *Comput. Mater. Sci.* **1999**, *14*, 8–12. (f) Sasaki, T.; Ohno, T. *Surf. Sci.* **1999**, *435*, 172–175. (g) Sasaki, T.; Ohno, T. *Surf. Sci.* **2000**, *454*, 337–340.

(17) Behler, J.; Delley, B.; Reuter, K.; Scheffler, M. *Phys. Rev. B* **2007**, *75*, 115409.

(18) Wodtke, A. M.; Matsiev, D.; Auerbach, D. J. *Prog. Surf. Sci.* **2008**, *83*, 167–214.
(19) Fan, X. L.; Lau, W. M.; Liu, Z. F. *Phys. Rev. Lett.* **2006**, *96*, 079801.
(20) Perdew, J. P.; Parr, R. G.; Levy, M.; Balduz, J. L. *Phys. Rev. Lett.* **1982**, *49*, 1691.
(21) Zhang, Y.; Yang, W. *J. Chem. Phys.* **1998**, *109*, 2604–2608.
(22) Baer, R.; Neuhauser, D. *Phys. Rev. Lett.* **2005**, *94*, 043002.
(23) Mosch, C.; Koukounas, C.; Bacalis, N.; Metropoulos, A.; Gross, A.; Mavridis, A. *J. Phys. Chem. C* **2008**, *112*, 6924–6932.
(24) Carbogno, C.; Behler, J.; Gross, A.; Reuter, K. *Phys. Rev. Lett.* **2008**, *101*.
(25) Perdew, J. P.; Burke, K.; Ernzerhof, M. *Phys. Rev. Lett.* **1996**, *77*, 3865–3868.
(26) (a) Lee, C. T.; Yang, W. T.; Parr, R. G. *Phys. Rev. B* **1988**, *37*, 785–789. (b) Becke, A. D. *J. Chem. Phys.* **1993**, *98*, 5648–5652.
(27) Livshits, E.; Baer, R. *Phys. Chem. Chem. Phys.* **2007**, *9*, 2932–2941.
(28) Livshits, E.; Baer, R. *J. Phys. Chem. A* **2008**, *112*, 12789.
(29) Savin, A. *Beyond the Kohn-Sham Determinant. In Recent Advances in Density Functional Methods Part I*; Chong, D. P., Ed.; World Scientific: Singapore, 1995; p 129.
(30) Iikura, H.; Tsuneda, T.; Yanai, T.; Hirao, K. *J. Chem. Phys.* **2001**, *115*, 3540–3544.
(31) (a) Kohn, W.; Sham, L. J. *Phys. Rev.* **1965**, *140*, A1133. (b) Hohenberg, P.; Kohn, W. *Phys. Rev.* **1964**, *136*, B864.
(32) Toulouse, J.; Colonna, F.; Savin, A. *Phys. Rev. A* **2004**, *70*, 062505.
(33) Levy, M.; Perdew, J. P. *Phys. Rev. A* **1985**, *32*, 2010–2021.
(34) Stein, T.; Kronik, L.; Baer, R. *J. Am. Chem. Soc.* **2009**, *131*, 2818.
(35) (a) Yanai, T.; Tew, D. P.; Handy, N. C. *Chem. Phys. Lett.* **2004**, *393*, 51. (b) Peach, M. J. G.; Helgaker, T.; Salek, P.; Keal, T. W.; Lutnaes, O. B.; Tozer, D. J.; Handy, N. C. *Phys. Chem. Chem. Phys.* **2006**, *8*, 558–562.
(36) Toulouse, J.; Savin, A.; Flad, H. J. *Int. J. Quantum Chem.* **2004**, *100*, 1047–1056.
(37) Shao, Y.; et al. *Phys. Chem. Chem. Phys.* **2006**, *8*, 3172–3191.
(38) (a) Ueno, J.; Hoshino, T.; Hata, M.; Tsuda, M. *Appl. Surf. Sci.* **2000**, *162*, 440–444. (b) Jones, R. O. *J. Chem. Phys.* **1993**, *99*, 1194–1206. (c) Sun, J.; Lu, W. C.; Wang, H.; Li, Z. S.; Sun, C. C. *J. Phys. Chem. A* **2006**, *110*, 2729–2738.
(39) Almbladh, C.-O.; von-Barth, U. *Phys. Rev. B* **1985**, *31*, 3231.
(40) Note the small oscilations of charge for the PBE is due to difficulties in converging the self consistent field calculation for PBE.
(41) Baer, R.; Livshits, E.; Neuhauser, D. *Chem. Phys.* **2006**, *329*, 266.
(42) Kümmel, S.; Kronik, L. *Rev. Mod. Phys.* **2008**, *80*, 3.
(43) Ervin, K. M.; Anusiewicz, W.; Skurski, P.; Simons, J.; Lineberger, W. C. *J. Phys. Chem. A* **2003**, *107*, 8521–8529.
(44) Drzaic, P. S.; Marks, J.; Brauman, J. I. In *Gas phase ion chemistry*; Bowers, M. T., Ed.; Academic Press: New York, 1984; p 167.
(45) Perdew, J. P.; Zunger, A. *Phys. Rev. B* **1981**, *23*, 5048.
(46) Ruzsinszky, A.; Perdew, J. P.; Csonka, G. I.; Vydrov, O. A.; Scuseria, G. E. *J. Chem. Phys.* **2007**, *126*, 104102.
(47) Krukau, A. V.; Scuseria, G. E.; Perdew, J. P.; Savin, A. *J. Chem. Phys.* **2008**, *129*, 124103–7.

JP900892R